




Tenomodulin and Chondromodulin-1 Are Both Required to Maintain Biomechanical Function and Prevent Intervertebral Disc Degeneration

CARTILAGE
2021, Vol. 13(Suppl 2) 604S–614S
© The Author(s) 2021
Article reuse guidelines:
sagepub.com/journals-permissions
DOI: 10.1177/19476035211029696
journals.sagepub.com/home/CAR
SAGE

Theodor Di Pauli von Treuheim^{1*} , Olivia M. Torre^{1*},
Emily D. Ferreri¹ , Philip Nasser¹, Angelica Abbondandolo¹,
Manuel Delgado Caceres², Dasheng Lin³ , Denitsa Docheva²,
and James C. Iatridis¹

Abstract

Objective. The underlying mechanisms and molecular factors influencing intervertebral disc (IVD) homeostasis and degeneration remain clinically relevant. Tenomodulin (Tnmd) and chondromodulin (Chm1) are antiangiogenic transmembrane glycoproteins, with cleavable C-terminus, expressed by IVD cells that are implicated in the onset of degenerative processes. We evaluate the organ-level biomechanical impact of knocking out Tnmd alone, and Tnmd and Chm1, simultaneously. **Design.** Caudal (c5-8) and lumbar vertebrae (L1-4) of skeletally mature male and female 9-month-old wildtype (WT), Tnmd knockout (Tnmd^{-/-}), and Tnmd/Chm1 double knockout (Tnmd^{-/-}/Chm1^{-/-}) mice were used ($n = 9-13$ per group). Disc height index (DHI), histomorphological changes, and axial, torsional, creep, and failure biomechanical properties were evaluated. Differences were assessed by one-way ANOVA with post hoc Bonferroni-corrected comparisons ($P < 0.05$). **Results.** Tnmd^{-/-}/Chm1^{-/-} IVDs displayed increased DHI and histomorphological scores that indicated increased IVD degeneration compared to the WT and Tnmd^{-/-} groups. Double knockout IVDs required significantly less torque and energy to initiate torsional failure. Creep parameters were comparable between all groups, except for the slow time constant, which indicated faster outward fluid flow. Tnmd^{-/-} IVDs lost fluid faster than the WT group, and this effect was amplified in the double knockout IVDs. **Conclusion.** Knocking out Tnmd and Chm1 affects IVD fluid flow and organ-level biomechanical function and therefore may play a role in contributing to IVD degeneration. Larger effects of the Tnmd and Chm1 double knockout mice compared to the Tnmd single mutant suggest that Chm1 may play a compensatory role in the Tnmd single mutant IVDs.

Keywords

intervertebral disc, biomechanics, tenomodulin, chondromodulin-1, structure function relationship

Introduction

Back pain is a leading cause of disability worldwide that is strongly associated with intervertebral disc (IVD) degeneration.¹⁻⁵ IVD degeneration is an aberrant, cell-mediated response to progressive structural failure⁶ with degradation of extracellular matrix molecules such as glycoproteins and collagen.^{7,8} Nucleus pulposus (NP) dehydration and decompression can cause damaging strains on the outer lamellar annulus fibrosus (AF) resulting in loss of IVD height and structural failure.^{6,9} Loss of NP pressurization and AF disruption can both result in IVD height loss and cause specific alterations to axial and torsional motion segment behaviors.⁹ IVDs heal poorly and can involve chronic pro-inflammatory conditions following structural disruption.^{10,11} The

¹Leni & Peter W. May Department of Orthopaedics, Icahn School of Medicine at Mount Sinai, New York, NY, USA

²Experimental Trauma Surgery, Department of Trauma Surgery, University Regensburg Medical Centre, Regensburg, Germany

³Orthopaedic Center of People's Liberation Army, The Affiliated Southeast Hospital of Xiamen University, Zhangzhou, China

*Authors contributed equally.

Supplementary material for this article is available on the *Cartilage* website at <https://journals.sagepub.com/home/car>.

Corresponding Author:

James C. Iatridis, Leni & Peter W. May Department of Orthopaedics, Icahn School of Medicine at Mount Sinai, One Gustave Levy Place, Box 1188, New York, NY 10029-6574, USA.

Email: theodor.dipaulivontreuheim@icahn.mssm.edu

accumulation of structural IVD disruption, IVD height loss, and chronic pro-inflammatory conditions characteristic of IVD degeneration can cause disability and pain. Disabling IVD degeneration-related pathologies are an important clinical challenge that motivate the investigation of structure-function relationships to identify important biomarkers of IVD homeostasis and promising therapeutic targets.

Tenomodulin (Tnmd) and chondromodulin I (Chm1) are 2 anti-angiogenic type II transmembrane glycoproteins with cleavable C-terminal domains secreted in the extracellular matrix. They have been reported to exert functional roles in hypovascular connective tissues such as tendons, cartilage, and IVDs.¹²⁻¹⁴ Tnmd is best-known as a tendon and ligament maturation marker.^{12,15,16} In tendon, *Tnmd* regulates tenocyte proliferation at neonatal stages, collagen fibril maturation, and scar formation during early healing.^{17,18} The role of *Tnmd* in the IVD is still emerging; it is expressed by human AF cells¹⁹ and is predominantly expressed by mouse outer AF cells.¹³ *Tnmd* deficient (*Tnmd*^{-/-}) mice demonstrated decreased AF collagen fibril diameter and nano-scale compressive stiffness, while increasing AF angiogenesis, macrophage infiltration of the outer AF, and hypertrophic-like chondrocytes in the NP.¹³ These changes resulted in IVD degeneration with a decrease in disc height index (DHI).¹³ *Chm1*, the only known homolog gene of *Tnmd*,^{13,15,16} could play compensatory roles in the maintenance of IVD structure and function. *Chm1* is expressed in both human and mice IVDs with major localization in the NP, and is believed to influence NP, AF, and endplate cell proliferation.^{13,20} More severe IVD degeneration and angiogenic disruption was observed in *Tnmd* and *Chm1* double knockout mice (*Tnmd*^{-/-}/*Chm1*^{-/-}) when compared to single knockout *Tnmd*^{-/-}.¹³

While *Tnmd* and *Chm1* are implicated in structural changes to IVDs, their roles on organ-level biomechanical function remain unclear. The objective of this study was to elucidate the roles of *Tnmd* and *Chm1* in IVD height, histomorphology, and IVD biomechanical function by knocking out *Tnmd* alone, or *Tnmd* and *Chm1* together. Axial and torsional biomechanical properties, as well as creep and torsional failure properties, were evaluated which together can distinguish effects on AF tension and NP pressurization.^{9,21} Since *Tnmd*^{-/-} IVDs showed decreased AF collagen fibril diameter and nano-scale compressive stiffness,¹³ we hypothesized that *Tnmd*^{-/-} and *Tnmd*^{-/-}/*Chm1*^{-/-} IVDs would display altered biomechanical properties due to AF collagen disruption, with more severe changes in the double knockout group.

Methods

Specimen Preparation

Skeletally mature female and male 9-month-old *Tnmd*^{-/-} mice and *Tnmd*^{+/+} wildtype (WT) or *Tnmd*^{+/-} heterozygous littermates, and *Tnmd*^{-/-}/*Chm1*^{-/-} mice were used in this study ($n = 9-13$ per group). WT and heterozygous

IVDs were grouped together as WT samples. The generation of *Tnmd*^{-/-} and *Tnmd*^{-/-}/*Chm1*^{-/-} mice genotype has been previously described.¹⁷ All mice were of a C57BL/6J background. After euthanasia with CO₂, caudal spines were collected and stored at -20 °C until testing. On testing day, tails were thawed in 1× phosphate-buffered saline (PBS) for 90 minutes at room temperature. Mouse husbandry, handling, and euthanasia were carried out strictly according to the guidelines of the Lower Franconia government.

Disc Height Index and Related Measurements

IVD height and vertebral body height were measured from caudal disc levels 5/6, 6/7, and 7/8 and averaged per specimen. Measurements were taken from anterior-posterior tail digital radiographs (UltraFocus, Faxitron) using established protocols.²² DHI was calculated from IVD and adjacent vertebral body measurements, as previously described.²³

Histomorphological Scoring

Histomorphological changes were assessed in lumbar disc levels 1/2-3/4 from specimens whose caudal discs underwent biomechanical testing. Histological preparation was performed in accordance with previously established protocols.¹³ In short, samples were fixed in 4% paraformaldehyde at 4 °C overnight, decalcified for 6 weeks in 10% ethylenediaminetetraacetic acid with PBS at a pH of 8.0, embedded in paraffin, sectioned at 6 μm, and stained with hematoxylin and eosin (H&E). Histomorphological scores were generated following newly developed scoring system, which characterizes structure, cellular infiltration, extent of mineralization, and evidence of clefts/fissures.^{13,24} The parameters evaluated were the following: NP structure (0 points, single-cell mass; 1 point, cell clusters <50%; 2 points, cell clusters >50%; 3 points, matrix-rich with little cells NP; 4 points, mineralized NP), NP clefts/fissures (0 points, none; 1 point, mild; 2 points, severe), AF/NP boundary (0 points, clear cut boundary; 1 point, round chondrocyte cells at the boundary; 2 points, loss of boundary), AF structure (0 points, concentric lamellar structure; 1 point, serpentine, widened, or rounded AF lamellae; 2 points, reversal of lamellae; 3 points, undefinable lamellar structure or penetrating the NP; 4 points, mineralized or lost AF), and AF clefts/fissures (0 points, none; 1 point, mild; 2 points, severe). For histological scoring, 6 *Tnmd*^{-/-} and 6 WT animals (3 IVDs/animal and 1 tissue section/IVD) were used. For the *Tnmd*^{-/-}/*Chm1*^{-/-} group, 5 animals (1 IVD/animal and 1 tissue section/IVD) were used.

Biomechanical Testing and Parameter Evaluation

Following the acquisition of caudal radiographs, caudal disc level 6/7 was dissected with adjacent vertebrae intact and the excess connective tissue removed (**Fig. 1**).

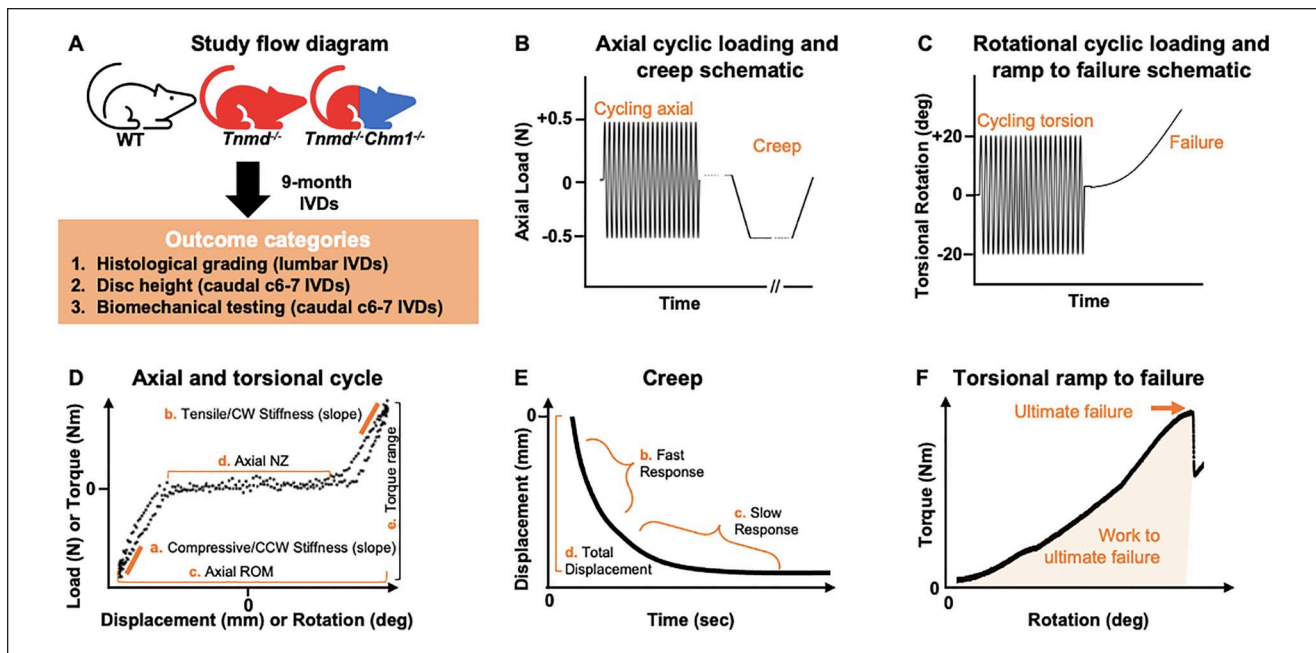


Figure 1. Study flow diagram with accompanying test protocols for axial tension/compression, creep, torsion, and torsional ramp to failure biomechanical parameters on representative loading curves. **(A)** Flow diagram illustrating the investigated outcome categories. **(B)** IVDs were subjected to 20 cycles of axial tension/compression at ± 0.5 N at 0.1 mm/second, then 45 minutes of creep at -0.5 N. **(C)** Following axial testing, IVDs were subjected to torsional testing starting with equilibrating for 5 minutes at a 0.1 MPa pre-load, then 20 cycles of torsion at $\pm 20^\circ$ at 0.5 Hz, and lastly 1° /second continuous rotation to failure. **(D)** Stiffness, ROM (range of motion), NZ (neutral zone), and torque range were determined from the 20th cycle of testing. **(E)** Creep parameters were obtained by fitting the raw data using previously described techniques.²⁹ **(F)** Ultimate failure was characterized as the peak torque of the first major failure event.³⁰

Mechanical behaviors of WT, *Tnmd*^{-/-}, and *Tnmd*^{-/-}/*Chm1*^{-/-} motion segments were assessed using custom axial (ELF3200, TA Instruments) and torsion (AR2000ex, TA Instruments) test systems following protocols as described previously.²⁵ WT, *Tnmd*^{-/-}, and *Tnmd*^{-/-}/*Chm1*^{-/-} motion segments were subjected to 20 cycles of axial tension/compression at ± 0.5 N at 0.1 mm/second, followed by 45 minutes of creep at -0.5 N (**Fig. 1B**). Following a 5-minute span of unloaded rehydration in a saline bath at room temperature, motion segments were subjected to torsional testing. Torsional testing began with 5-minute equilibration at 0.1 MPa pre-load, followed by 20 cycles of torsion at $\pm 20^\circ$ cycling at 0.5 Hz, and finally continuous torsion to failure at a rate of 1° /second (**Fig. 1C**).

Axial data were analyzed for compressive and tensile elastic zone (EZ) stiffness, range of motion (ROM), and neutral zone (NZ) length from the 20th cycle using a custom MATLAB program²⁶ (MathWorks; **Fig. 1D**). Compressive and tensile EZ stiffness were calculated as a linear fit to 90% to 100% of maximum load when plotted against displacement. Axial ROM was calculated as the total displacement from compression to tension. Axial NZ length was defined as the portion of the load-displacement curve where motion was produced with minimal resistance²⁷ and was measured from the load versus

displacement curve using a custom MATLAB script, employing the double sigmoid method.^{25,26,28}

Torsional data were analyzed for torque range and torsional stiffness from the 20th cycle (**Fig. 1D**). Torsional stiffness in the clockwise (CW) and counterclockwise (CCW) directions was averaged to obtain a single value. Torsional stiffness was calculated as a linear fit to 90% to 100% of the loading direction torque versus rotation curve and reported as an average of CW and CCW directions. Torque range was calculated as the total torque developed from fully CW to fully CCW rotations.

Creep data were analyzed for elastic response stiffness (S_e), fast response stiffness (S_1), slow response stiffness (S_2), fast time constant (τ_1), slow time constant (τ_2), and total creep displacement (**Fig. 1E**), as previously described.²⁹

Torsional failure data were analyzed for ultimate failure torque, work to ultimate failure, and ultimate failure degree (**Fig. 1F**). These metrics were recorded at the instant where ultimate failure occurred based on rotation versus torque plots, using previously characterized definitions constituting a failure event.³⁰ The failure event was therefore not terminated based on visual cues, but rather permitted to complete its scheduled protocol since visual inspection was unreliable in pilot test runs. All values from these biomechanical tests were calculated using a custom MATLAB program.²⁶

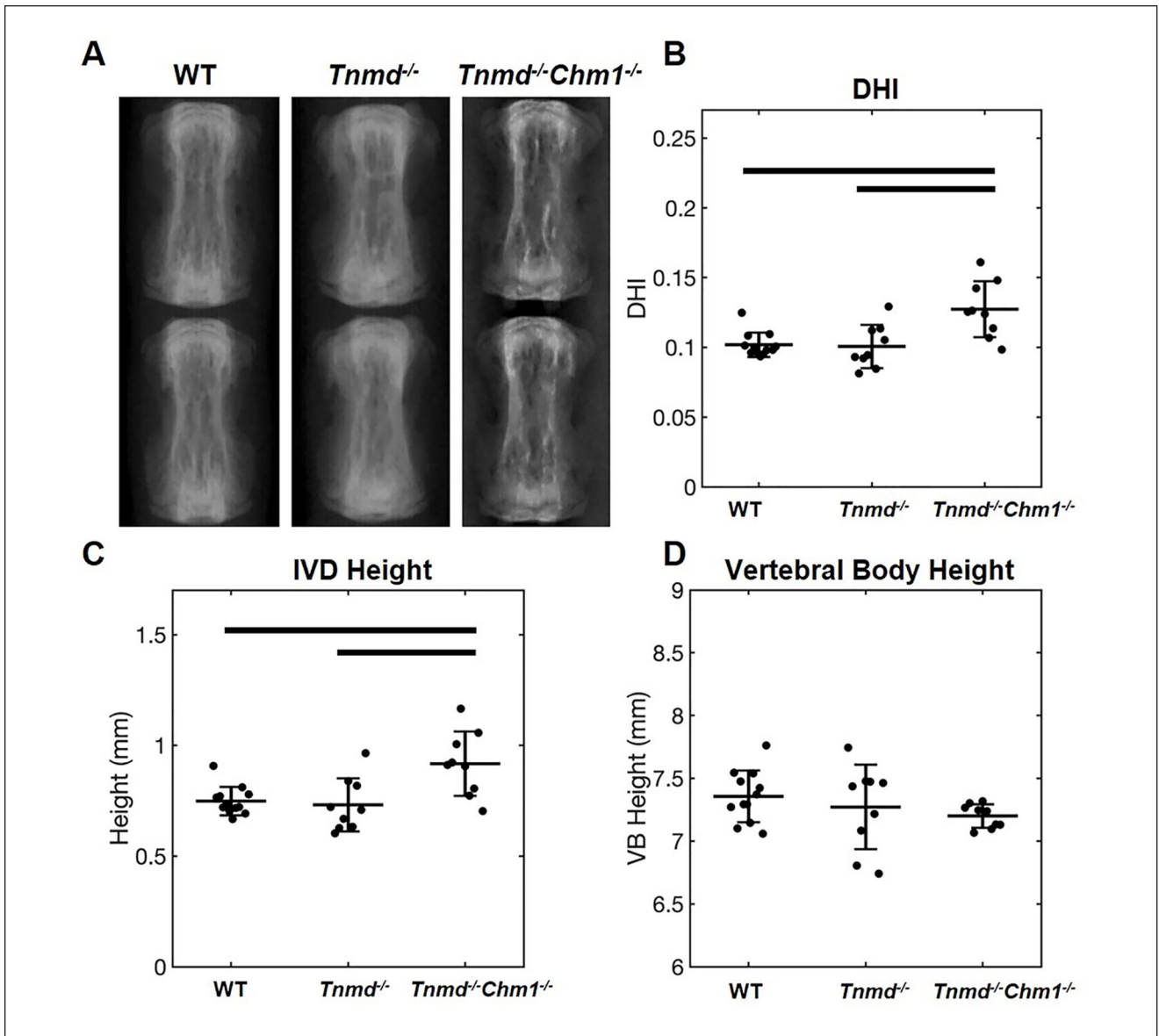


Figure 2. Effect of *Tnmd*^{-/-} and *Tnmd*^{-/-}/*Chm1*^{-/-} on DHI in skeletally mature caudal IVDs. **(A)** Representative radiographs of WT, *Tnmd*^{-/-}, and *Tnmd*^{-/-}/*Chm1*^{-/-} caudal spines (level 6/7 shown). **(B-D)** Quantification of DHI, IVD height, and vertebral body height show an increase in DHI and IVD height for *Tnmd*^{-/-}/*Chm1*^{-/-} compared to *Tnmd*^{-/-} and WT, but no changes in vertebral body height. Solid bars indicate *P* < 0.05.

Statistics

One-way ANOVA with *post hoc* Bonferroni correction for multiple group comparisons determined the role of *Tnmd*^{-/-} and *Tnmd*^{-/-}/*Chm1*^{-/-} on DHI, histomorphological score, and biomechanical parameters with *P* < 0.05 denoting statistical significance. Outliers were removed using MATLAB if distributing beyond 3 scaled median absolute deviations from the median. Prism (GraphPad) and MATLAB were used to generate figures.

Results

DHI in Caudal IVDs Was Increased for Tnmd^{-/-}/*Chm1*^{-/-} Mice

No differences were found for caudal vertebral body height across all 3 groups, and no differences were found in caudal IVD height and DHI between WT and *Tnmd*^{-/-} specimen. *Tnmd*^{-/-}/*Chm1*^{-/-} specimens resulted in significantly larger caudal IVD height and DHI compared to WT and *Tnmd*^{-/-} groups (**Fig. 2**).

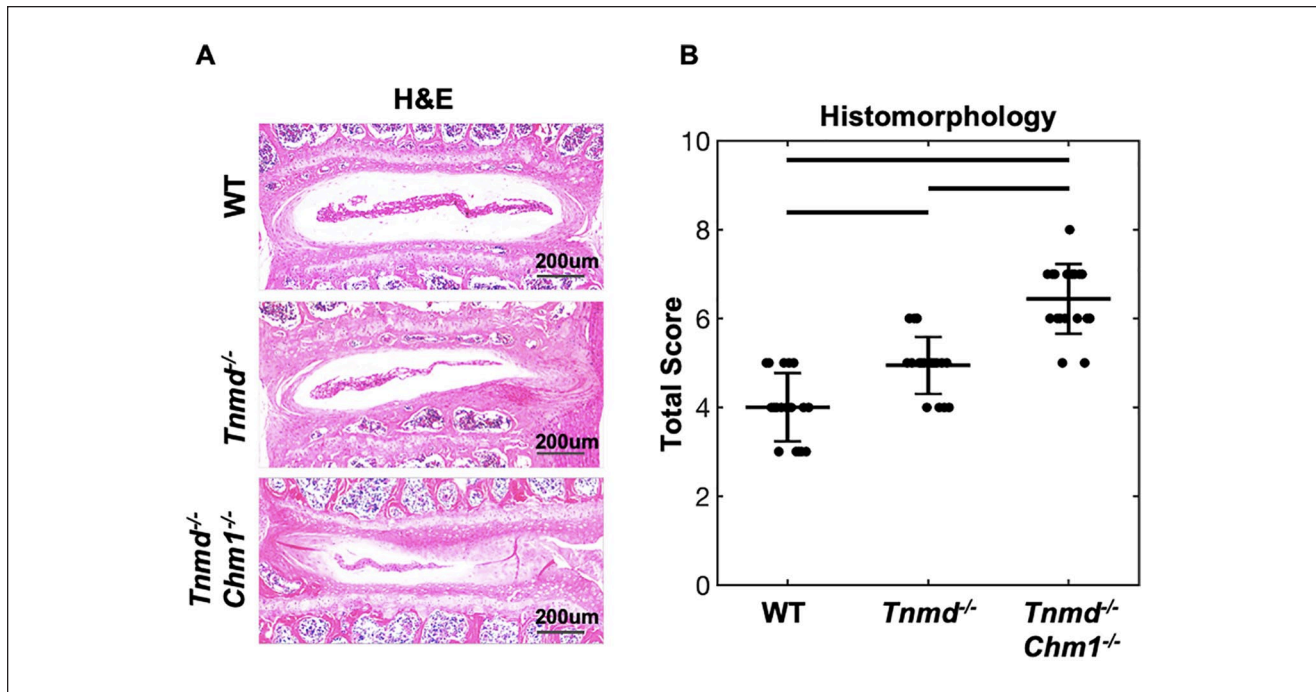


Figure 3. Histomorphological scoring of WT, *Tnmd*^{-/-}, and *Tnmd*^{-/-}/*Chm1*^{-/-} lumbar IVDs. **(A)** Representative images of WT, *Tnmd*^{-/-}, and *Tnmd*^{-/-}/*Chm1*^{-/-} IVDs stained with H&E. **(B)** Quantification of changes in AF and NP structure, cellular infiltration, clefts/fissures, lamellar orientation, and mineralization show an increase in histological score for *Tnmd*^{-/-}/*Chm1*^{-/-} compared to WT and *Tnmd*^{-/-} groups. Scale bar = 200 μ m. Solid bars indicate $P < 0.05$ and interrupted bars indicate $P = 0.08$.

Histomorphological Degeneration Scores in Lumbar IVDs Were Increased for *Chm1*^{-/-}/*Tnmd*^{-/-} Mice

Histomorphological scores quantified NP and AF features by aggregating IVD characteristics, including cell clusters, extent of mineralization, clefts/fissures, and lamellar structure of 9-month-old lumbar IVDs. The WT group had the lowest score, with histological degeneration progressively increasing when knocking out *Tnmd* alone ($P = 0.08$) and increasing further when both *Tnmd* and *Chm1* ($P = 0.001$) were deficient (**Fig. 3**). When compared directly to the WT by *t*-test, the single knockout was significantly increased ($P = 0.019$). H&E staining revealed fewer NP cells and matrix concomitant with poor lamellar structure penetrating the NP in *Tnmd*^{-/-} IVDs. In *Tnmd*^{-/-}/*Chm1*^{-/-} mice, more severe IVD degeneration, associated with larger NP penetration, AF fissures, and loss of AF lamellar morphology, was observed.

Axial and Torsional Biomechanical Function of Caudal IVDs Was Affected More by *Tnmd*^{-/-}/*Chm1*^{-/-} Than *Tnmd*^{-/-} Alone

Axial compressive stiffness, but not tensile stiffness, was significantly increased for *Tnmd*^{-/-}/*Chm1*^{-/-} compared to

WT and *Tnmd*^{-/-} (**Fig. 4A and B**). Axial ROM of *Tnmd*^{-/-} and *Tnmd*^{-/-}/*Chm1*^{-/-} were decreased relative to WT, although it did not reach statistical significance ($P = 0.05$) (**Fig. 4C**). Axial NZ and torsional parameters were unchanged between groups (**Fig. 4D-F**).

Creep Testing of Caudal IVDs Determined Slow Creep Time Constant Was Affected by *Tnmd*^{-/-}/*Chm1*^{-/-}

Creep stiffness parameters S_c , S_1 , and S_2 , were unchanged between groups (**Fig. 5A-C**). Slow creep time constant (τ_2) was significantly decreased in *Tnmd*^{-/-}/*Chm1*^{-/-} and decreased ($P = 0.05$) in *Tnmd*^{-/-} IVDs, while the fast time constant (τ_1) was unchanged between groups (**Fig. 5D and E**). Total disc creep displacement was similar between all groups (WT: 0.16 ± 0.03 mm; *Tnmd*^{-/-}: 0.17 ± 0.01 mm; *Tnmd*^{-/-}/*Chm1*^{-/-}: 0.17 ± 0.01 mm) (**Fig. 5F**).

Torsional Failure Properties of Caudal IVDs Were Affected by *Tnmd*^{-/-}/*Chm1*^{-/-}

Tnmd^{-/-}/*Chm1*^{-/-} IVDs had decreased ultimate failure torque, work to failure, and degree at which failure occurred when compared to WT and *Tnmd*^{-/-} groups (**Fig. 6A-C**). *Tnmd*^{-/-}/*Chm1*^{-/-} IVDs failed at a lesser degree of rotation,

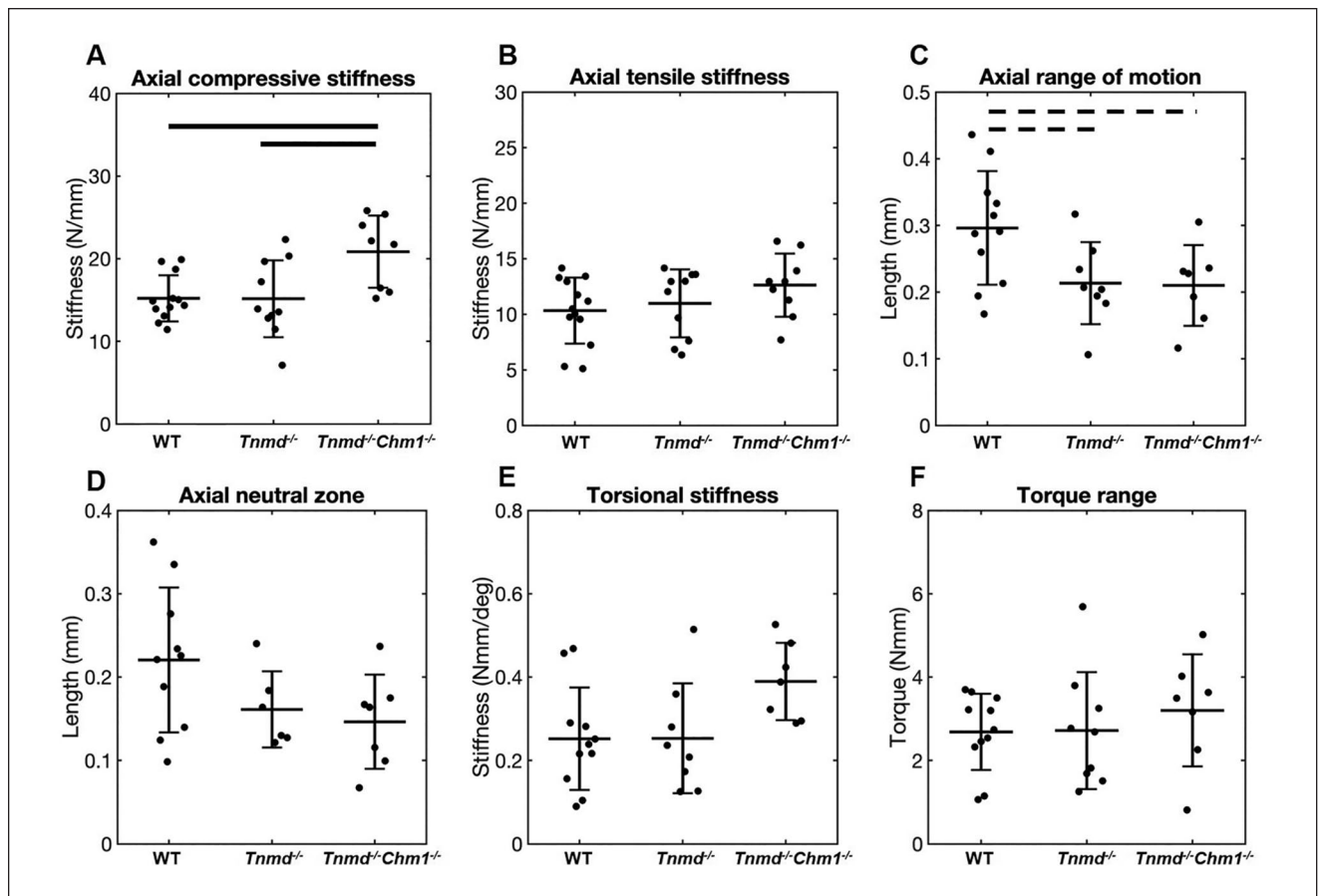


Figure 4. Effect of *Tnmd*^{-/-} and *Tnmd*^{-/-}/*Chm1*^{-/-} on axial and torsional parameters. **(A)** Axial compressive stiffness increased for *Tnmd*^{-/-}/*Chm1*^{-/-} compared to *Tnmd*^{-/-} and WT. **(B-F)** All other parameters showed no significant differences between groups, but *Tnmd*^{-/-} and *Tnmd*^{-/-}/*Chm1*^{-/-} trended toward lower values for ROM compared to WT. Solid bars indicate *P* < 0.05, interrupted bars indicate *P* = 0.05.

requiring significantly less torque and energy (work) to cause failure. By allowing the failure protocol to run to completion, gross inspection captured failure which occurred mostly at the endplates and at the outer AF in the mid-disc axial plane (**Fig. 6D**). The single *Tnmd*^{-/-} IVDs did not demonstrate differences in torsional failure parameters compared to WT IVDs (**Fig. 6A-C**).

Discussion

In order to determine the contribution of *Tnmd* and *Chm1* on organ-level IVD motion segment function we characterized DHI (caudal IVDs), IVD histomorphology (lumbar IVDs), and biomechanical parameters (caudal IVDs) in WT, *Tnmd*^{-/-}, and *Tnmd*^{-/-}/*Chm1*^{-/-} mice. Double knockout *Tnmd*^{-/-}/*Chm1*^{-/-} IVDs displayed significantly increased DHI, histomorphological degeneration scores, and axial compressive stiffness, and a decrease in creep slow time constant (τ_2) and all torsional failure parameters. Single knockout *Tnmd*^{-/-} IVDs were minimally impacted across

these variables, suggesting *Chm1* compensates for IVD organ-level biomechanical function when *Tnmd* is absent. The reduced torsional failure strength and decreased τ_2 suggest AF collagen disruption was enhanced in the double knockout compared to the single knockout, and results suggest collagen disruption led to endplate contact which increased compressive stiffness. IVDs lacking *Tnmd* and *Chm1* were previously shown to accelerate degenerative processes as measured by molecular markers,¹³ and we now add to this knowledge by demonstrating that their deficiency increased degenerative processes with diminished inferior load carriage and fluid transport.

Viscoelastic compressive creep findings showed that the slow time constant τ_2 was decreased in *Tnmd*^{-/-} and *Tnmd*^{-/-}/*Chm1*^{-/-} mice, while other creep variables were unaffected (**Fig. 5**). Decreased τ_2 is primarily associated with increased fluid transport out of the IVD due to increased tissue permeability.²⁹ Creep loading results depend on preconditioning, which was satisfied by our axial cyclic loading test prior to the creep test. Furthermore, achieving intradiscal pressure

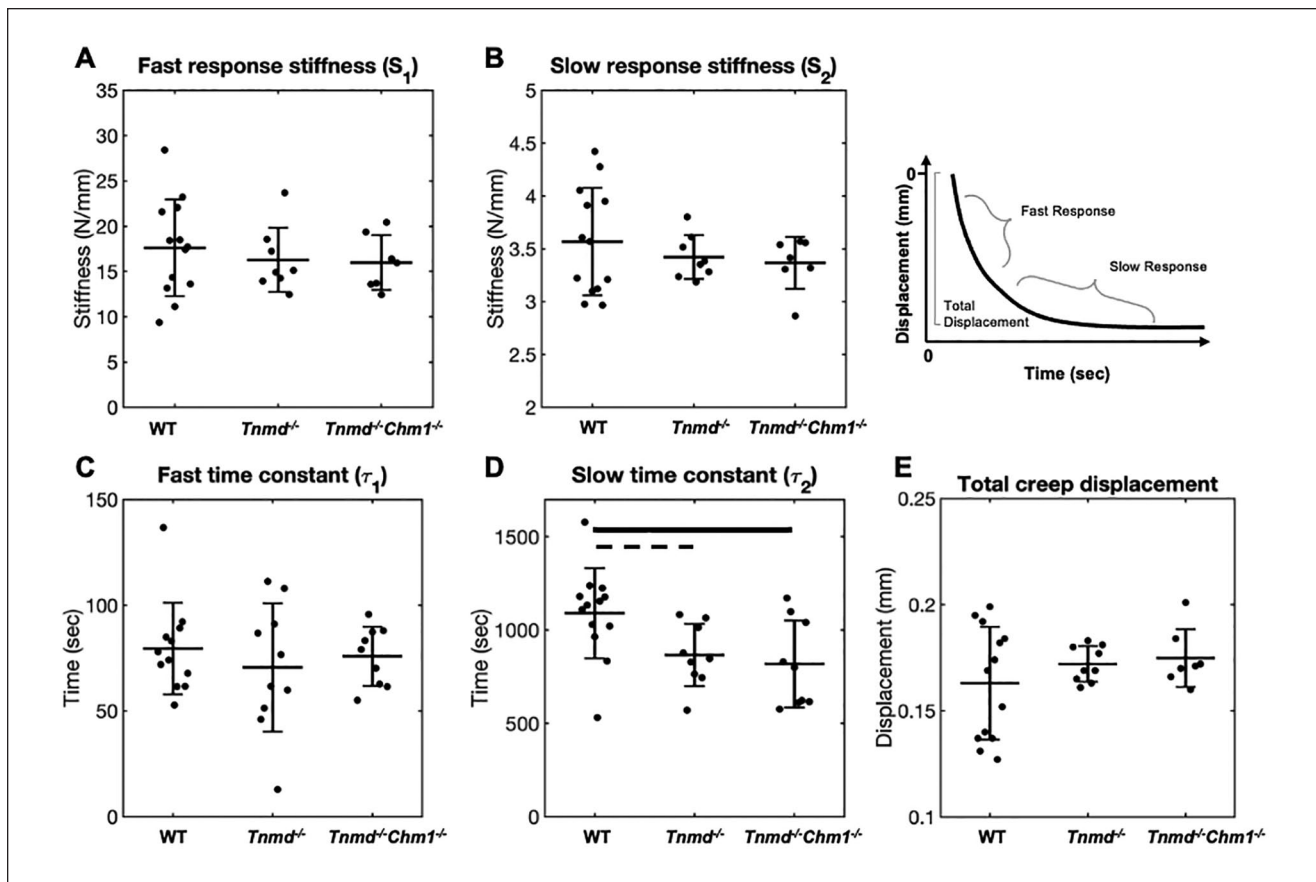


Figure 5. Effect of *Tnmd*^{-/-} and *Tnmd*^{-/-}/*Chm1*^{-/-} on creep parameters. (A-C) S_e , S_1 , and S_2 were unchanged between groups. (D, E) τ_2 , but not τ_1 , was significantly reduced in *Tnmd*^{-/-}/*Chm1*^{-/-} and almost significantly reduced ($P = 0.05$) in *Tnmd*^{-/-} compared to WT. (F) Total creep displacement was similar between groups, with greater variability in WT. Solid bars indicate $P < 0.05$, interrupted bars indicate $P = 0.05$.

equilibrium in murine specimen occurs after approximately 20 minutes, granting confidence in our slow time constant results.^{21,31} We propose that *Tnmd* and *Chm1* deficiency increases fluid transport due to disrupted AF collagen structure. This inference is based on the findings that the *Tnmd* protein co-localizes with type I collagen,³² where *Tnmd* deficiency caused decreased AF collagen fibril diameter,¹³ and decreased collagen fibril diameter is associated with increased fluid transport.³³ In tendons, lack of *Tnmd* also decreased expression of genes related to collagen crosslinking,³² where decreased crosslinking also correlated with decreased flow resistance.³⁴ Consequently, the faster fluid transport out of the IVD (as evidenced by decreased τ_2) may also have resulted from disrupted AF collagen crosslinking from *Tnmd* deficiency. In human, fluid permeability is reported to be unaffected, increased, and decreased by IVD degeneration.^{29,35-37} These competing findings may be explained by the various degenerative stages, defects, and disease conditions that accumulate over decades in humans³⁸ and can differentially influence fluid transport

and biomechanical function.³⁹ Taken in the context of this broader literature, we infer that even relatively minor collagen disruptions as might occur from *Tnmd* and *Chm1* deficiency can diminish creep behaviors and alter load carriage that may accumulate in degenerative changes. We also conclude that *Tnmd* and *Chm1* deficiency disrupted AF collagen fibril network, which resulted in more rapid fluid outflow during compressive creep.

Tnmd and *Chm1* deficiency increased the histomorphological degenerative grade of lumbar IVDs and altered DHI of caudal IVDs. In humans, IVD height loss is an early sign of degeneration that can occur from alterations in AF integrity or NP pressurization.^{9,39} Pro-angiogenic factors increase under pathological conditions, encouraging IVD vascularity and calcification of cartilaginous tissues.⁴⁰ *Tnmd* and *Chm1* are known anti-angiogenic proteins, and therefore increased histomorphological scores (via increased mineralization) corroborates their roles as potential affectors of early degenerative processes. The increase in score compared to the WT when *Tnmd* alone was knocked out was not

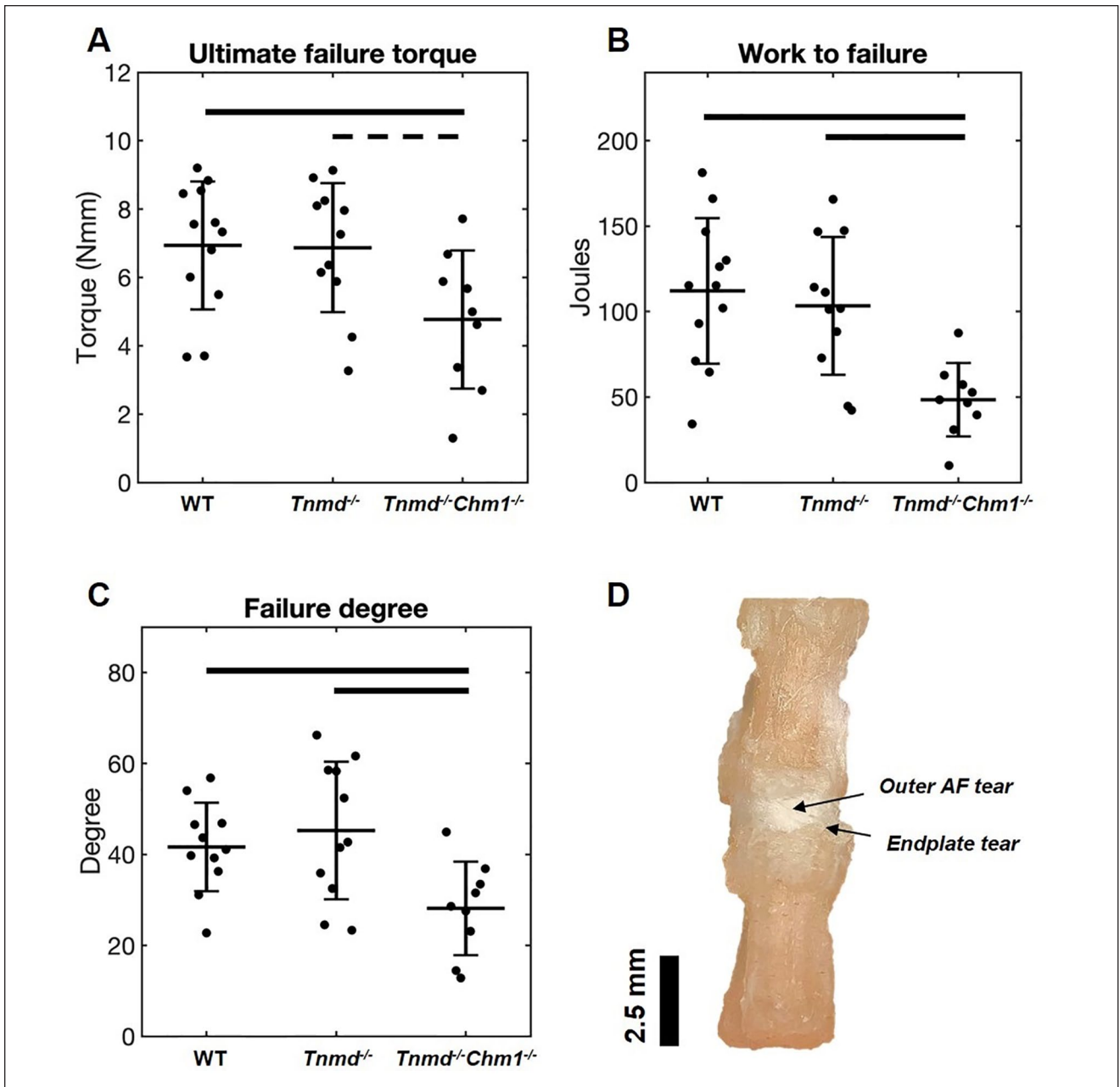


Figure 6. Effect of *Tnmd*^{-/-} and *Tnmd*^{-/-}/*Chm1*^{-/-} on torsional failure parameters. **(A)** Mean ultimate failure torque decreased for *Tnmd*^{-/-}/*Chm1*^{-/-} compared to WT and trended toward a decrease compared to *Tnmd*^{-/-}. **(B and C)** Work to failure and failure degree decreased for *Tnmd*^{-/-}/*Chm1*^{-/-} compared to WT and *Tnmd*^{-/-}. **(D)** Gross examination of most failure events showed fissuring of outer AF and tear at the endplate. Solid bars indicate $P < 0.05$, interrupted bars indicate $P = 0.05$.

statistically significant due to corrections from multiple pairwise analyses. However, a direct comparison between *Tnmd*^{-/-} and WT parallels results previously reported in 6- and 12-month-old mice showing increased degenerative scores secondary to *Tnmd* deficiency.¹³ In the same study, DHI measurements using histological sections showed decreased DHI of lumbar IVDs in *Tnmd*^{-/-} IVDs. However, this current study shows increased DHI in *Tnmd*^{-/-}

Chm1^{-/-} IVDs. These contradictory findings are most likely related to differences in spinal levels used and specimen preparation differences. Lumbar segments were used in a prior study,¹³ where histological preparation dehydrates tissues, possibly causing endplates to converge and leading to decreased DHI, especially if collagen is disrupted. The current study measured caudal IVD and vertebral dimensions in whole mouse tails via radiographs where saline-soaked

tissues that maintained hydration conditions can cause swelling during specimen handling and imaging, especially if collagen is disrupted. It is also possible that collagen disruption would cause an increase in DHI in caudal levels and decrease in DHI in lumbar levels *in vivo* because peak forces are lower on caudal levels than on lumbar spinal levels. Since both studies and methods are well controlled, we conclude that both studies point to collagen disruption that influence DHI.

This study demonstrated that *Tnmd*^{-/-}/*Chm1*^{-/-} IVDs had significantly increased axial compressive stiffness, which is commonly associated with NP pressurization but can also be influenced by changes in AF collagen.⁹ Loss of proteoglycans can result in NP depressurization, decreased IVD height, and altered axial biomechanical properties.^{9,41,42} However, *Tnmd* is primarily expressed in the outer AF¹³ without a known influence on proteoglycans in tendons.¹⁷ The increased compressive stiffness in this study may therefore be attributed to sudden stiffening from endplate-to-endplate contact due to AF collagen disruption. Premature endplate-to-endplate contact occurs with NP depressurization, which can happen in the setting of disrupted collagen integrity, resulting a sudden load increase when endplates contact. The axial test protocol used in this study involved displacement-control to a maximum load-limit, which can result in increased stiffness as endplate contact generates the load-limit with lower deformation. Our chosen schema provided the highest possible sensitivity to detect an effect and was deemed appropriate given that 75% of the spine biomechanics community agrees that the loading schema should be applied based on the research question.²¹ We note that micro-scale modulus measured with atomic force microscopy was decreased in *Tnmd*^{-/-} IVDs compared to WT IVDs and this test more directly measures the local extracellular matrix without interacting structures that comprise the motion segment.¹³ We therefore attribute premature endplate-to-endplate contact as the mechanism responsible for our axial compression organ-level results.

The torsion to failure biomechanical test identified that significantly reduced torque and work were required to generate a failure when both *Tnmd* and *Chm1* were deficient. Torsional parameters are highly sensitive and specific to AF disruption,³⁰ and torsional failure in this study occurred in the outer AF and at its endplate insertion. The AF contains primarily a type 1 collagen network, which is responsible for resisting motion segment torsion.⁴³ *Tnmd* is predominantly expressed in the outer AF,¹³ whereas *Chm1* is mostly localized to the NP but influences cell populations of the NP, AF, and endplate.¹³ Torsional failure properties of this study were only affected by the double knockout, suggesting that *Chm1* influences cell populations involved in AF lamellar architecture and can maintain AF structural integrity in the absence of *Tnmd*. It was somewhat surprising that torsional failure properties were diminished while torsional

stiffness was not affected, and we attribute this to the complex lamellar architecture of the AF that permits redundancy in lamellar layers.⁴⁴ Furthermore, it highlights that *Tnmd* and *Chm1* cause relatively minor alterations that were most detectable when forcing rotation beyond 20° (which was the maximum rotation during cyclic torsion testing).

The use of mice models enables genetic modifications, and mice and human IVDs have similar axial and torsional mechanical properties when normalized by size.^{45,46} Organ level biomechanical changes were sensitive enough to detect collagen changes in *Tnmd*^{-/-}/*Chm1*^{-/-} but not *Tnmd*^{-/-} which was previously reported to have collagen disruption detectable with micro-scale mechanics measured with atomic force microscopy.¹³ Motion segment tests evaluate functional biomechanical changes involve multiple interacting structures but have less sensitivity than atomic force microscopy measurements, which are highly sensitive to biomechanical changes on the micro-scale and can be localized to AF extracellular matrix. While we can conclude that *Tnmd* and *Chm1* play interacting roles, this study did not have a single *Chm1* knockout subgroup, which prevents making conclusions on the synergistic, permissive, or independent roles of *Chm1* and *Tnmd*.

This study identified that *Tnmd* and *Chm1* are both required to maintain IVD organ-level biomechanical integrity. *Tnmd* homolog *Chm1* may serve a compensatory role, evidenced by our finding that only the double knockout genotype generated biomechanical phenotypic changes. *Tnmd* and *Chm1* had direct effects on early IVD degeneration, increased fluid transport, and outer AF collagen disruption. Future studies are warranted to identify the directionality of the relationship between these proteins that contribute to the AF phenotype. These factors may also serve as biomarkers of IVD degeneration or help inform AF repair strategies.

Author Contributions

Theodor Di Pauli von Treuheim: Planned and conceptualized the study, wrote MATLAB program, analyzed and interpreted data, wrote and edited the manuscript, and approved the final version.

Olivia M. Torre: Planned and conceptualized the study, interpreted data, led collaboration communications, and approved the final version.

Emily D. Ferreri: X-ray testing and analysis, wrote and edited the manuscript, and approved the final version manuscript writing.

Philip Nasser: Experimental set up and resource allocation.

Angelica Abbondandolo: X-ray analysis.

Manuel Delgado Caceres: IVD explantation, collaboration, communications, and reviewed, edited, and approved the manuscript.

Dasheng Lin: Histological preparation and assessment.

Denitsa Docheva: Planned and conceptualized the study, interpreted the results, and reviewed, edited, and approved the manuscript.

James C. Iatridis: Planned and conceptualized the study, interpreted the results, and reviewed, edited, and approved the manuscript.

Acknowledgments and Funding

The author(s) disclosed receipt of the following financial support for the research, authorship, and/or publication of this article: This work was supported by R01AR057397 (JCI) from NIH/NIAMS and the EU Twinning Grant ACHILLES (H2020-WIDESPREAD-05-2017-Twinning Grant No. 810850) (DD). The investigators thank Dr. Zsuzsa Jenei-Lanzl for histological support on lumbar IVD specimens.

Declaration of Conflicting Interests

The author(s) declared no potential conflicts of interest with respect to the research, authorship, and/or publication of this article.

Ethical Approval

Ethical approval for this study was obtained from the Lower Franconia ethics committee.

Animal Welfare

The present study followed international, national, and/or institutional guidelines for humane animal treatment and complied with relevant legislation.

ORCID iDs

Theodor Di Pauli von Treuheim  <https://orcid.org/0000-0002-7281-9758>

Emily D. Ferreri  <https://orcid.org/0000-0001-7298-4801>

Dasheng Lin  <https://orcid.org/0000-0003-4568-2044>

References

- Murray CJL, Atkinson C, Bhalla K, Birbeck G, Burstein R, Chou D, *et al.* The state of US health, 1990-2010: burden of diseases, injuries, and risk factors. *JAMA*. 2013;310(6):591-608. doi:10.1001/jama.2013.13805
- Vos T, Flaxman AD, Naghavi M, Lozano R, Michaud C, Ezzati M, *et al.* Years lived with disability (YLDs) for 1160 sequelae of 289 diseases and injuries 1990-2010: a systematic analysis for the Global Burden of Disease Study 2010. *Lancet*. 2012;380(9859):2163-96. doi:10.1016/S0140-6736(12)61729-2
- Luoma K, Riihimäki H, Luukkonen R, Raininko R, Viikari-Juntura E, Lamminen A. Low back pain in relation to lumbar disc degeneration. *Spine (Phila Pa 1976)*. 2000;25(4):487-92. doi:10.1097/00007632-200002150-00016
- Luoma K, Vehmas T, Kerttula L, Grönblad M, Rinne E. Chronic low back pain in relation to Modic changes, bony endplate lesions, and disc degeneration in a prospective MRI study. *Eur Spine J*. 2016;25(9):2873-81. doi:10.1007/s00586-016-4715-x
- Livshits G, Popham M, Malkin I, Sambrook PN, Macgregor AJ, Spector T, *et al.* Lumbar disc degeneration and genetic factors are the main risk factors for low back pain in women: the UK Twin Spine Study. *Ann Rheum Dis*. 2011;70(10):1740-5. doi:10.1136/ard.2010.137836
- Adams MA, Roughley PJ. What is intervertebral disc degeneration, and what causes it? *Spine (Phila Pa 1976)*. 2006;31(18):2151-61. doi:10.1097/01.brs.0000231761.73859.2c
- Antoniou J, Steffen T, Nelson F, Winterbottom N, Hollander AP, Poole RA, *et al.* The human lumbar intervertebral disc: evidence for changes in the biosynthesis and denaturation of the extracellular matrix with growth, maturation, ageing, and degeneration. *J Clin Invest*. 1996;98(4):996-1003. doi:10.1172/JCI118884
- Buckwalter JA. Aging and degeneration of the human intervertebral disc. *Spine (Phila Pa 1976)*. 1995;20(11):1307-14. doi:10.1097/00007632-199506000-00022
- Iatridis JC, Nicoll SB, Michalek AJ, Walter BA, Gupta MS. Role of biomechanics in intervertebral disc degeneration and regenerative therapies: what needs repairing in the disc and what are promising biomaterials for its repair? *Spine J*. 2013;13(3):243-62. doi:10.1016/j.spinee.2012.12.002
- Risbud MV, Shapiro IM. Role of cytokines in intervertebral disc degeneration: pain and disc content. *Nat Rev Rheumatol*. 2014;10(1):44-56. doi:10.1038/nrrheum.2013.160
- Huang YC, Urban JPG, Luk KDK. Intervertebral disc regeneration: do nutrients lead the way? *Nat Rev Rheumatol*. 2014;10(9):561-6. doi:10.1038/nrrheum.2014.91
- Dex S, Lin D, Shukunami C, Docheva D. Tenogenic modulating insider factor: systematic assessment on the functions of tenomodulin gene. *Gene*. 2016;587(1):1-17. doi:10.1016/j.gene.2016.04.051
- Lin D, Alberton P, Caceres MD, Prein C, Clausen-Schaumann H, Dong J, *et al.* Loss of tenomodulin expression is a risk factor for age-related intervertebral disc degeneration. *Aging Cell*. 2020;19(3):e13091. doi:10.1111/ace1.13091
- Shukunami C, Hiraki Y. Chondromodulin-I and tenomodulin: the negative control of angiogenesis in connective tissue. *Curr Pharm Des*. 2007;13(20):2101-12. doi:10.2174/138161207781039751
- Brandau O, Meindl A, Fässler R, Aszódi A. A novel gene, *tendin*, is strongly expressed in tendons and ligaments and shows high homology with chondromodulin-I. *Dev Dyn*. 2001;221(1):72-80. doi:10.1002/dvdy.1126
- Shukunami C, Oshima Y, Hiraki Y. Molecular cloning of tenomodulin, a novel chondromodulin-I related gene. *Biochem Biophys Res Commun*. 2001;280(5):1323-7. doi:10.1006/bbrc.2001.4271
- Docheva D, Hunziker EB, Fässler R, Brandau O. Tenomodulin is necessary for tenocyte proliferation and tendon maturation. *Mol Cell Biol*. 2005;25(2):699-705. doi:10.1128/MCB.25.2.699-705.2005
- Lin D, Alberton P, Caceres MD, Volkmer E, Schieker M, Docheva D. Tenomodulin is essential for prevention of adipocyte accumulation and fibrovascular scar formation during early tendon healing. *Cell Death Dis*. 2017;8(10):e3116. doi:10.1038/cddis.2017.510
- Minogue BM, Richardson SM, Zeef LA, Freemont AJ, Hoyland JA. Transcriptional profiling of bovine intervertebral disc cells: implications for identification of normal and degenerate human intervertebral disc cell phenotypes. *Arthritis Res Ther*. 2010;12(1):R22. doi:10.1186/ar2929
- Takao T, Iwaki T, Kondo J, Hiraki Y. Immunohistochemistry of chondromodulin-I in the human intervertebral discs with special reference to the degenerative changes. *Histochem J*. 2000;32(9):545-50. doi:10.1023/a:1004150211097
- Costi JJ, Ledet EH, O'Connell GD. Spine biomechanical testing methodologies: the controversy of consensus vs

- scientific evidence. *JOR Spine*. 2021;5(4):e1138. doi:10.1002/jsp2.1138
22. Torre OM, Das R, Berenblum RE, Huang AH, Iatridis JC. Neonatal mouse intervertebral discs heal with restored function following herniation injury. *FASEB J*. 2018;32(9):4753-62. doi:10.1096/fj.201701492R
 23. Masuda K, Aota Y, Muehleman C, Imai Y, Okuma M, Thonar EJ, *et al*. A novel rabbit model of mild, reproducible disc degeneration by an annulus needle puncture: correlation between the degree of disc injury and radiological and histological appearances of disc degeneration. *Spine (Phila Pa 1976)*. 2005;30(1):5-14. doi:10.1097/01.brs.0000148152.04401.20
 24. Tam V, Chan WCW, Leung VYL, Cheah KSE, Cheung KMC, Sakai D, *et al*. Histological and reference system for the analysis of mouse intervertebral disc. *J Orthop Res*. 2018;36(1):233-43. doi:10.1002/jor.23637
 25. Torre OM, Evashwick-Rogler TW, Nasser P, Iatridis JC. Biomechanical test protocols to detect minor injury effects in intervertebral discs. *J Mech Behav Biomed Mater*. 2019;95:13-20. doi:10.1016/j.jmbbm.2019.03.024
 26. Di Pauli von Treuheim T, Torre OM, Mosley GE, Nasser P, Iatridis JC. Measuring the neutral zone of spinal motion segments: comparison of multiple analysis methods to quantify spinal instability. *JOR Spine*. 2020;3(2):e1088. doi:10.1002/jsp2.1088
 27. Panjabi MM. The stabilizing system of the spine. Part II. Neutral zone and instability hypothesis. *J Spinal Disord*. 1992;5(4):390-7. doi:10.1097/00002517-199212000-00002
 28. Smit TH, van Tunen MS, van der Veen AJ, Kingma I, van Dieën JH. Quantifying intervertebral disc mechanics: a new definition of the neutral zone. *BMC Musculoskelet Disord*. 2011;12:38. doi:10.1186/1471-2474-12-38
 29. O'Connell GD, Jacobs NT, Sen S, Vresilovic EJ, Elliott DM. Axial creep loading and unloaded recovery of the human intervertebral disc and the effect of degeneration. *J Mech Behav Biomed Mater*. 2011;4(7):933-42. doi:10.1016/j.jmbbm.2011.02.002
 30. Michalek AJ, Iatridis JC. Height and torsional stiffness are most sensitive to annular injury in large animal intervertebral discs. *Spine J*. 2012;12(5):425-32. doi:10.1016/j.spinee.2012.04.001
 31. Palmer EI, Lotz JC. The compressive creep properties of normal and degenerated murine intervertebral discs. *J Orthop Res*. 2004;22(1):164-9. doi:10.1016/S0736-0266(03)00161-X
 32. Dex S, Alberton P, Willkomm L, Sollradl T, Bago S, Milz S, *et al*. Tenomodulin is required for tendon endurance running and collagen I fibril adaptation to mechanical load. *EBioMedicine*. 2017;20:240-54. doi:10.1016/j.ebiom.2017.05.003
 33. Olsson PO, Gustafsson R, In't Zandt R, Friman T, Maccarana M, Tykesson E, *et al*. The tyrosine kinase inhibitor imatinib augments extracellular fluid exchange and reduces average collagen fibril diameter in experimental carcinoma. *Mol Cancer Ther*. 2016;15(10):2455-64. doi:10.1158/1535-7163.MCT-16-0026
 34. Kapellos GE, Alexiou TS. Modeling momentum and mass transport in cellular biological media: from the molecular to the tissue scale. In: *Transport in Biological Media*. Elsevier; 2013:1-40. doi:10.1016/B978-0-12-415824-5.00001-1
 35. Gu WY, Mao XG, Foster RJ, Weidenbaum M, Mow VC, Rawlins BA. The anisotropic hydraulic permeability of human lumbar annulus fibrosus. Influence of age, degeneration, direction, and water content. *Spine (Phila Pa 1976)*. 1999;24(23):2449-55. doi:10.1097/00007632-199912010-00005
 36. Antoniou J, Epure LM, Michalek AJ, Grant MP, Iatridis JC, Mwale F. Analysis of quantitative magnetic resonance imaging and biomechanical parameters on human discs with different grades of degeneration. *J Magn Reson Imaging*. 2013;38(6):1402-14. doi:10.1002/jmri.24120
 37. Iatridis JC, Setton LA, Foster RJ, Rawlins BA, Weidenbaum M, Mow VC. Degeneration affects the anisotropic and nonlinear behaviors of human annulus fibrosus in compression. *J Biomech*. 1998;31(6):535-44. doi:10.1016/S0021-9290(98)00046-3
 38. Walter BA, Torre OM, Laudier D, Naidich TP, Hecht AC, Iatridis JC. Form and function of the intervertebral disc in health and disease: a morphological and stain comparison study. *J Anat*. 2015;227(6):707-16. doi:10.1111/joa.12258
 39. Volkheimer D, Galbusera F, Liebsch C, Schlegel S, Rohlmann F, Kleiner S, *et al*. Is intervertebral disc degeneration related to segmental instability? An evaluation with two different grading systems based on clinical imaging. *Acta Radiol*. 2018;59(3):327-35. doi:10.1177/0284185117715284
 40. Cornejo MC, Cho SK, Giannarelli C, Iatridis JC, Purmessur D. Soluble factors from the notochordal-rich intervertebral disc inhibit endothelial cell invasion and vessel formation in the presence and absence of pro-inflammatory cytokines. *Osteoarthritis Cartilage*. 2015;23(3):487-96. doi:10.1016/j.joca.2014.12.010
 41. Foltz MH, Kage CC, Johnson CP, Ellingson AM. Noninvasive assessment of biochemical and mechanical properties of lumbar discs through quantitative magnetic resonance imaging in asymptomatic volunteers. *J Biomech Eng*. 2017;139(11):1110021-7. doi:10.1115/1.4037549
 42. Yang B, O'Connell GD. Intervertebral disc swelling maintains strain homeostasis throughout the annulus fibrosus: a finite element analysis of healthy and degenerated discs. *Acta Biomater*. 2019;100:61-74. doi:10.1016/j.actbio.2019.09.035
 43. Torre OM, Mroz V, Bartelstein MK, Huang AH, Iatridis JC. Annulus fibrosus cell phenotypes in homeostasis and injury: implications for regenerative strategies. *Ann N Y Acad Sci*. 2019;1442(1):61-78. doi:10.1111/nyas.13964
 44. Iatridis JC, Ap Gwynn I. Mechanisms for mechanical damage in the intervertebral disc annulus fibrosus. *J Biomech*. 2004;37(8):1165-75. doi:10.1016/j.jbiomech.2003.12.026
 45. Showalter BL, Beckstein JC, Martin JT, Beattie EE, Orias AAE, Schaer TP, *et al*. Comparison of animal discs used in disc research to human lumbar disc: torsion mechanics and collagen content. *Spine (Phila Pa 1976)*. 2012;37(15):E900-E907. doi:10.1097/BRS.0b013e31824d911c
 46. Beckstein JC, Sen S, Schaer TP, Vresilovic EJ, Elliott DM. Comparison of animal discs used in disc research to human lumbar disc. *Spine (Phila Pa 1976)*. 2008;33(6):E166-E173. doi:10.1097/BRS.0b013e318166e001